

Electronic supplementary information (ESI)

Microstructure tuned $\text{Na}_3\text{V}_2(\text{PO}_4)_3@C$ electrodes toward ultra-long life sodium-ion batteries

Ranjit S. Kate^{a,b}, Kaustav Bhattacharjee^b, Milind V. Kulkarni^b, Ramesh J. Deokate^{a*}, Bharat B. Kale^{b,c*}, Ramchandra S. Kalubarme^{b*}

^a*Vidya Pratishthan's Arts, Science and Commerce College, Vidyanagari, Baramati 413 133, India*

^b*Centre for Materials for Electronics Technology, Panchavati, Off. Dr. Homi Bhabha Road, Pashan Pune -411 008, India.*

^c*MIT World Peace University (MIT-WPU), Kothrud, Pune 411 038, India.*

Corresponding Author: Dr. Ramchandra S. Kalubarme, Email: ram.kalubarme@cmet.gov.in

Dr. Ramesh J. Deokate, Email: rjdeokate@gmail.com

Dr. Bharat B. Kale, Email: bbkale@cmet.gov.in

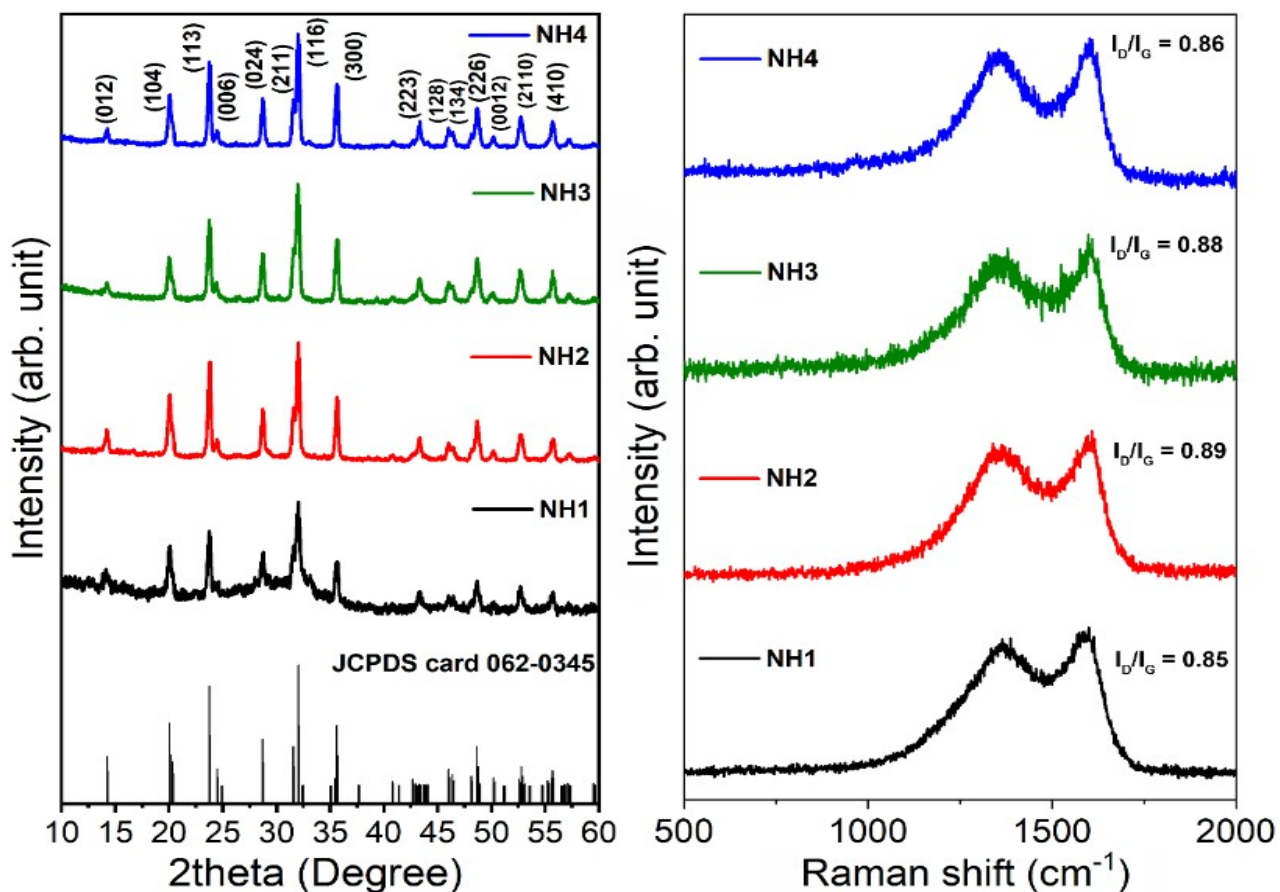


Fig. S1 (a) Powder X-ray diffraction patterns of different NVP@C samples along with the relevant JCPDS reference pattern. (b) Raman spectra of different NVP@C samples.

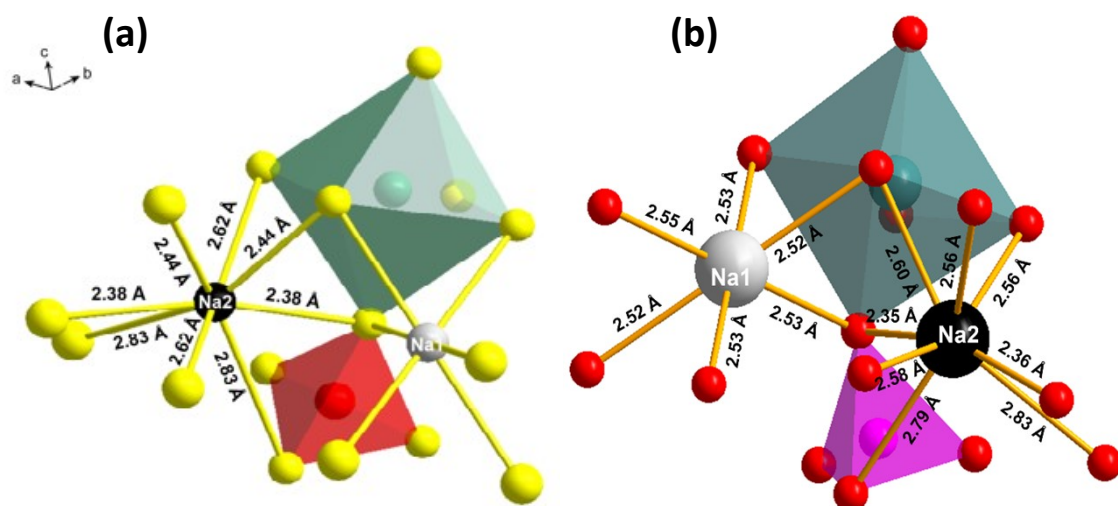


Fig. S2 (a) A representative molecular fragment showing different Na-sites and their coordination number (CN) of the standard $\text{Na}_3\text{V}_2(\text{PO}_4)_3$ (COD: 2225132), (b) $\text{Na}_3\text{V}_2(\text{PO}_4)_3$ sample calcined at 850°C .

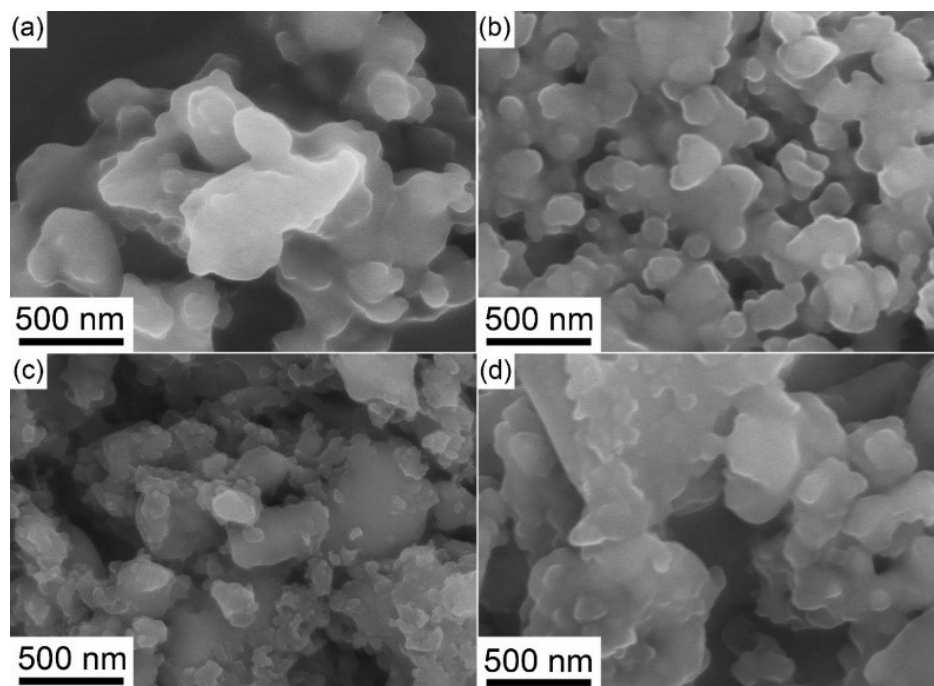


Fig. S3 FESEM images of NVP@C at different calcination temperatures: 750°C (a), 800°C (b), 850°C (c), and 900°C (d).

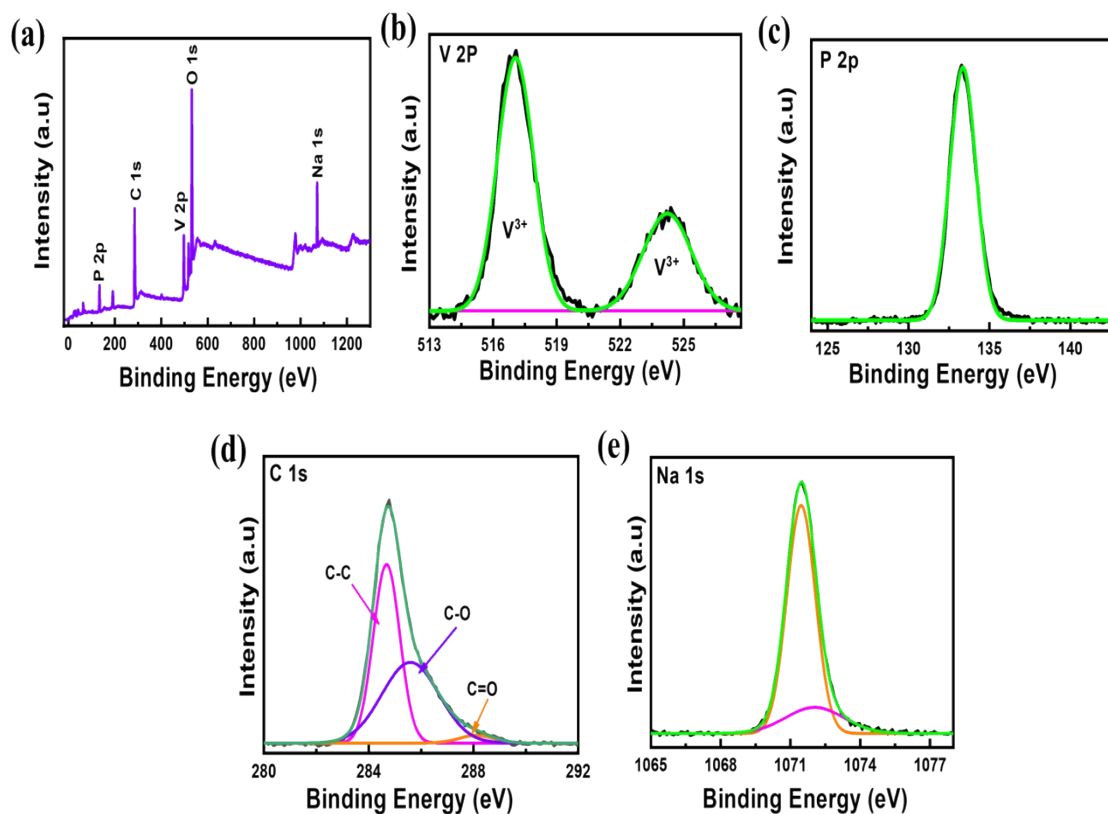


Fig. S4 XPS spectra of NVP@C calcined at 850°C (a) survey spectrum, (b) V 2p, (c) P 2p, (d) C 1s, and (e) Na 1s.

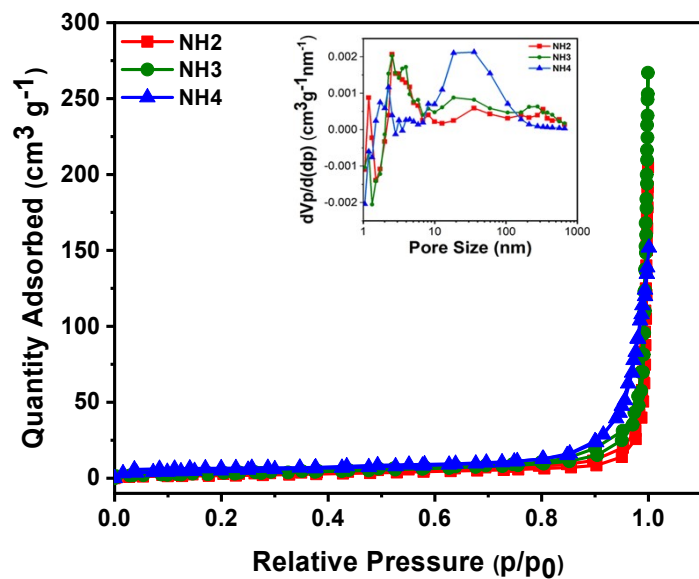


Fig. S5 N₂ Adsorption–desorption isotherm of NVP@C at different calcination temperatures.

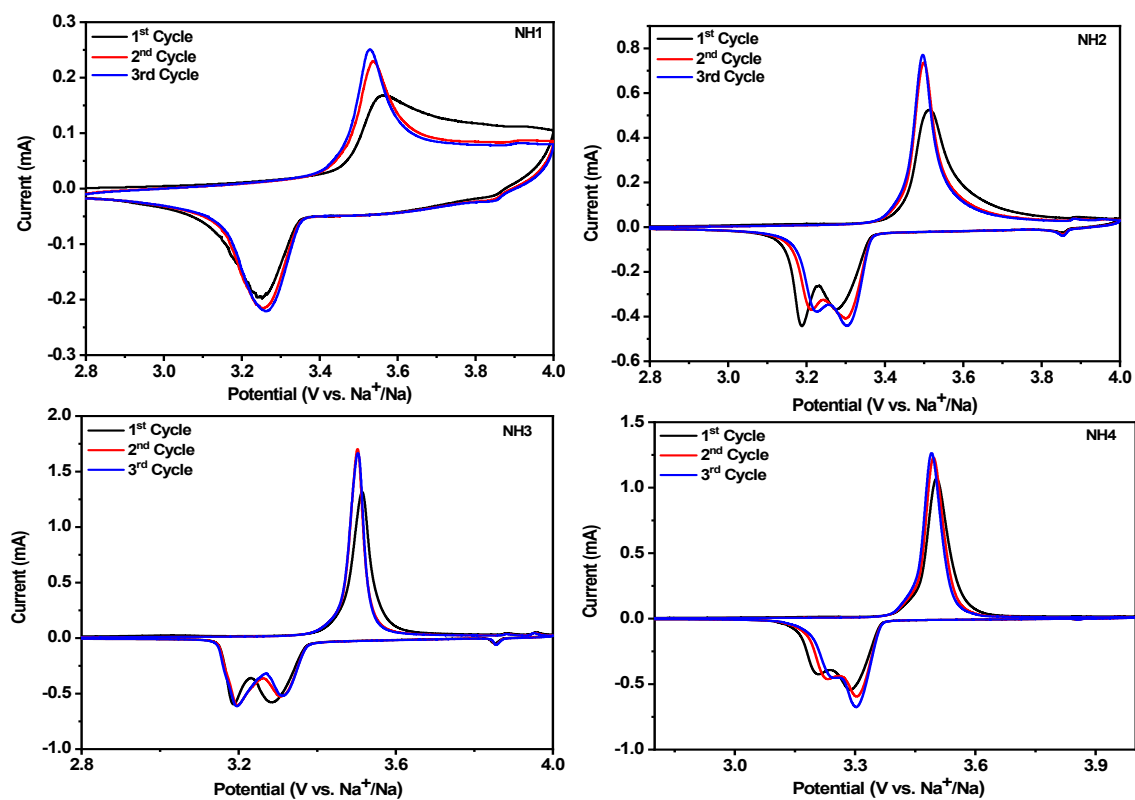


Fig.S6 CV curves of NVP@C at different calcination temperatures.

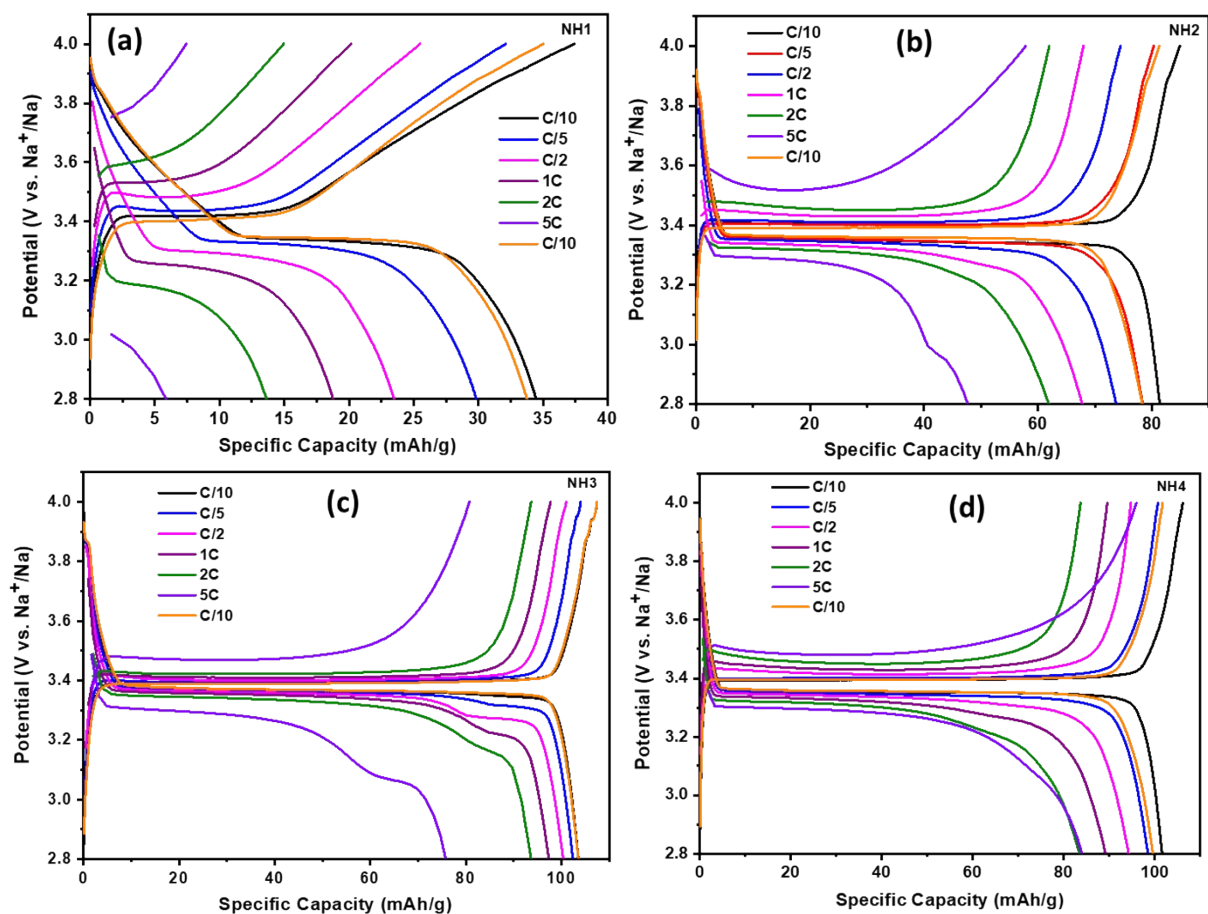


Fig.S7 The first charge-discharge profiles at different current rates of NVP@C at different calcination temperatures in a potential range of 2.8–4.0 V vs. Na/Na⁺ (a) 750, (b) 800, (c) 850 and (d) 900°C.

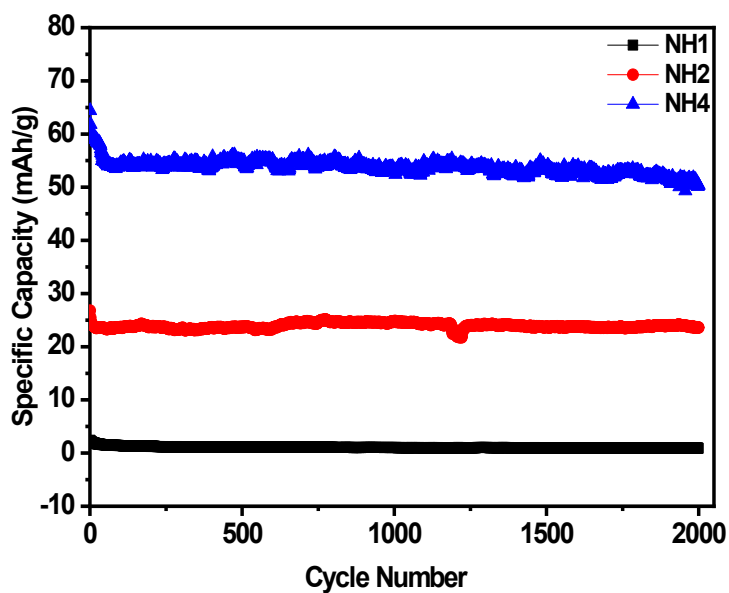


Fig. S8 Cycling performance of NVP@C calcined at 750, 800 & 900°C.

Table S1: Different crystal structure parameters used in the PXRD refinement analysis for the NH3 sample.

Symbol	Multiplicity	Wyckoff	x/a	y/b	z/c	Occupancy
Na1	6	b	0.3333	0.6666	0.1667	0.8144
Na2	18	e	0.6667	0.9838	0.0833	0.7205
O1	36	f	0.1501	0.5012	0.0830	0.9783
O2	36	f	0.5594	0.8402	0.9744	-0.0252
P	18	e	-0.0363	0.3333	0.0833	1.0481
V	12	c	0.3333	0.6666	0.0169	0.9895

Table S2. BET surface area, pore radius, and pore volume of NVP@C for different calcination temperatures.

Sample	Surface area (m ² g ⁻¹)	Average Pore radius (nm)	Pore Volume (cc g ⁻¹)
NH2	9	48	0.2254
NH3	13	46	0.3020
NH4	17	24	0.2091

Table S3. Oxidation/reduction peaks and potential differences for different calcination temperatures.

Temperature (°C)	Peak Position (V) 1 st cycle		Peak Position (V) 3 rd cycle		Potential difference (V) 1 st cycle	Potential difference (V) 3 rd cycle
	Oxidation	Reduction	Oxidation	Reduction		
750	3.55	3.24	3.52	3.26	0.31	0.26
800	3.51	3.28 & 3.19	3.49	3.30 & 3.22	0.23	0.19
850	3.51	3.28 & 3.18	3.50	3.31 & 3.19	0.23	0.19
900	3.50	3.29 & 3.20	3.49	3.30 & 3.23	0.21	0.19

Table S4. Comparison of Specific discharge capacities for the first four cycles at different C-rates and temperatures.

Temperature (°C)	Specific Capacities (mAh g ⁻¹)						
	C/10	C/5	C/2	1C	2C	5C	C/10
750	34	29	23	18	13	6-5	33
800	82-81	79-78	78-74	72-68	62	47-46	78
850	103	103-102	100	98-97	94-93	75	103
900	101	100-98	94	90-89	84-83	84-81	99

Table S5. The comparison of electrochemical performances of $\text{Na}_3\text{V}_2(\text{PO}_4)_3$ -based cathode materials.

Electrode	C-rate	Discharge Capacity (mAh g^{-1}) (Cycle Number)	Capacity Retention	Ref.
NVP/C	10C	63	-	[1]
NVP/C	10C	62 (1) – 38 (3000)	62%	[2]
NVP/C	10C	84.4	-	[3]
NVP-C-B0.38%	10C	87 (1) – 70 (50)	80.9%	[4]
NVP/C nanowire	1C	94 (1)-20 (50)	53.2%	[5]
NVP/(C+G)	5C	95.3 (1)-88.7 (200)	92.5%	[6]
$\text{Na}_3\text{V}_2(\text{PO}_4)_3/\text{C}$	10C	≈ 40	-	[7]
$\text{Na}_3\text{V}_2(\text{PO}_4)_3/\text{C}$	10C	25	-	[8]
NVP/G	5C	86 (1)-70 (50)	70%	[9]
$\text{Na}_3\text{V}_2(\text{PO}_4)_3/\text{C}$	10C	92 (1)-72 (100)	77.8%	[10]
$\text{Na}_3\text{V}_2(\text{PO}_4)_3/\text{C}$	1C	70 (1)-50 (200)	80%	[11]
$\text{Na}_3\text{V}_2(\text{PO}_4)_3/\text{C}$	1C	100 (1)-45 (400)	45%	[12]
Br/N/a-C@NVP	10C	40 (1)-32 (500)	92%	[13]
NVP@N-HC	10C	93 (1)-67 (1000)	72%	[14]
3D NVP@C	5C	81 (1)-76 (200)	94.2%	[15]
NVP@C nanofiber	2 C	77 (4)-75 (66)	97.4%	[16]
NVP@PEDOT	1C	100 (1)-80 (200)	80%	[17]
Fe-NVP@C	5C	91 (1)-43 (400)	46.7%	[18]
$\text{Na}_3\text{V}_2(\text{PO}_4)_3/\text{C}$	10C	64 (1)-52 (1000)	81.5%	[19]
$\text{Na}_3\text{V}_2(\text{PO}_4)_3/\text{C}$	10C	67 (1)-63 (2000)	94%	Current Work

References:

- [1] H. Li, Y. Bai, F. Wu, Q. Ni, C. Wu, $\text{Na}_3\text{V}_2(\text{PO}_4)_3/\text{C}$ nanorods as advanced cathode material for sodium ion batteries, *Solid State Ionics*, 2015, **278**, 281–286.
- [2] D. X. Wang, N. Chen, M. L. Li, C. Z. Wang, E. Helmut, X. F. Bie, Y. J. Wei, G. Chen, F. Du, $\text{Na}_3\text{V}_2(\text{PO}_4)_3/\text{C}$ Composite as the Intercalation-Type Anode Material for Sodium-Ion Batteries with Superior Rate Capability and Long-Cycle Life, *J. Mater. Chem. A*, 2015, **3**, 8636-8642.
- [3] H. Wang, D.L. Jiang, Y. Zhang, G.P. Li, X.Z. Lan, H.H. Zhong, Z.P. Zhang, Y. Jiang, Self-combustion synthesis of $\text{Na}_3\text{V}_2(\text{PO}_4)_3$ nanoparticles coated with carbon shell as cathode materials for sodium-ion batteries, *Electrochim. Acta*, 2015, **155**, 23–28.

- [4] W. Shen, H. Li, C. Wang, Z. H. Li, Q. J. Xu, H. M. Liu, Y. G. Wang, Improved Electrochemical Performance of the $\text{Na}_3\text{V}_2(\text{PO}_4)_3$ Cathode by B-Doping of the Carbon Coating layer for Sodium-Ion Batteries, *J. Mater. Chem. A*, 2015, **3**, 15190-15201.
- [5] S. Kajiyama, J. Kikkawa, J. Hoshino, M. Okubo, E. Hosono, Assembly of $\text{Na}_3\text{V}_2(\text{PO}_4)_3$ Nanoparticles Confined in a One-Dimensional Carbon Sheath for Enhanced Sodium-Ion Cathode Properties, *Chemistry A European Journal*, 2014, **20**, 12636-12640.
- [6] Z.L. Chu, C.B. Yue, Graphene oxide wrapped $\text{Na}_3\text{V}_2(\text{PO}_4)_3/\text{C}$ nanocomposite as superior cathode material for sodium-ion batteries, *Ceram. Int.*, 2016, **42**, 820–827.
- [7] J. Liu, K. Tang, K. Song, P. A. van Aken, Y. Yu, and J. Maier, Electrospun $\text{Na}_3\text{V}_2(\text{PO}_4)_3/\text{C}$ nanofibers as stable cathode materials for sodium-ion batteries, *Nanoscale*, 2014, **6**, 5081-5086.
- [8] H. Zhou, Z. Ryan Tian, S. S. Ang, Improving the cycling stability of $\text{Na}_3\text{V}_2(\text{PO}_4)_3$ nanoparticle in aqueous sodium-ion batteries by introducing carbon support, *Mater Renew Sustain Energy*, 2016, **5**, 1-9.
- [9] D. Guo, J. Qin, Z. Yin, J. Bai, Y. Sun, M. Cao, Achieving high mass loading of $\text{Na}_3\text{V}_2(\text{PO}_4)_3$ @carbon on carbon cloth by constructing three-dimensional network between carbon fibers for ultralong cycle-life and ultrahigh rate sodium-ion batteries, *Nano Energy*, 2018, **45**, 136-147.
- [10] H. Chen, Y. Huang, G. Mao, H. Tong, W. Yu, J. Zheng, and Z. Ding, Reduced Graphene Oxide Decorated $\text{Na}_3\text{V}_2(\text{PO}_4)_3$ Microspheres as Cathode Material With Advanced Sodium Storage Performance, *Front. Chem.*, 2018, **6**, 1-8.
- [11] C. Huang, Z. Zuo, J. Deng, Q. Yao, Z. Wang, H. Zhou, Electrochemical Properties of Hollow Spherical $\text{Na}_3\text{V}_2(\text{PO}_4)_3/\text{C}$ Cathode Materials for Sodium-ion Batteries, *Int. J. Electrochem. Sci.*, 2017, **12**, 9456 – 9464.
- [12] S. Tao, P. Cui, W. Huang, Z. Yu, X. Wang, S. Wei, D. Liu, L. Song, W. Chu, Sol-gel design strategy for embedded $\text{Na}_3\text{V}_2(\text{PO}_4)_3$ particles into carbon matrices for high-performance sodium-ion batteries, *Carbon*, 2016, **96**, 1028-1033.
- [13] Z. Wang, J. Liu, Z. Du, H. Tao, and Y. Yue, Enhancing Na-ion storage in $\text{Na}_3\text{V}_2(\text{PO}_4)_3/\text{C}$ cathodes for sodium-ion batteries through Br and N co-doping, *Inorg. Chem. Front.*, 2020, **7**, 1289-1297.
- [14] K. Sun, Y. B. Hu, X. D. Zhang, K. S. Hui, K. L. Zhang, G. G. Xu, J. Y. Ma, W. N. He, Doped Hard/Soft Double-Carbon-Coated $\text{Na}_3\text{V}_2(\text{PO}_4)_3$ Hybrid-Porous Microspheres with Pseudocapacitive Behaviour for Ultrahigh Power Sodium-Ion Batteries, *Electrochim. Acta*, 2020, **335**, 135680-135692.

- [15] Q. Zhang, W. Wang, Y. J. Wang, P. Y. Feng, K. L. Wang, S. J. Cheng, K. Jiang, Controllable Construction of 3D-Skeleton-Carbon Coated $\text{Na}_3\text{V}_2(\text{PO}_4)_3$ for High-Performance Sodium-Ion Battery cathode, *Nano Energy*, 2015, **20**, 11-19.
- [16] J. Liu, K. Tang, K. P. Song, A. V. A. Peter, Y. Yu, M. Joachim, Electrospun $\text{Na}_3\text{V}_2(\text{PO}_4)_3/\text{C}$ Nanofibers as Stable Cathode Materials for Sodium-Ion. Batteries, *Nanoscale*, 2014, **6**, 5081-5086.
- [17] J. X. Zhang, T. C. Yuan, H. Y. Wan, J. F. Qian, X. P. Ai, H. X. Yang, Y. L. Cao, Surface-Engineering Enhanced Sodium Storage Performance of $\text{Na}_3\text{V}_2(\text{PO}_4)_3$ Cathode via in-situ Self-Decorated Conducting Polymer Route, *Science China Chemistry* 2017, **60**, 1546-1553.
- [18] X. H. Liu, G. L. Feng, E. H. Wang, H. Chen, Z. G. Wu, W. Xiang, Y. J. Zhong, Y. X. Chen, X. D. Guo, B. H. Zhong, Insight into Preparation of Fe-Doped $\text{Na}_3\text{V}_2(\text{PO}_4)_3@\text{C}$ from Aspects of Particle Morphology Design, Crystal Structure Modulation, and Carbon Graphitization Regulation, *ACS Appl. Mater. Interfaces.*, 2019, **11**, 12421-12430.
- [19] N. Li, Y. Tong, D. Yi, X. Cui, X. Zhang, 3D interconnected porous carbon-coated $\text{Na}_3\text{V}_2(\text{PO}_4)_3/\text{C}$ composite cathode materials for sodium-ion batteries, *Ceramics International*, 2020, **46**, 27493-27498.